arXiv:0906.4214v2 [hep-ex] 9 Nov 2009

Measurement of cross sections of exclusive $e^+e^- \to VP$ processes at $\sqrt{s} = 10.58$ GeV

(Belle Collaboration)

K. Belous[12], M. Shapkin[12], I. Adachi[9], H. Aihara[43], K. Arinstein[1,32], V. Aulchenko[1,32], A. M. Bakich[39], V. Balagura[14], E. Barberio[22], W. Bartel[9], A. Bay[19], M. Bischofberger[24], A. Bondar[1,32], A. Bozek[28], M. Bračko[21,15], T. E. Browder[8], P. Chang[27], Y. Chao[27], A. Chen[25], B. G. Cheon[7], I.-S. Cho[47], S.-K. Choi[6], Y. Choi[38], J. Dalseno[9], M. Dash[46], A. Drutskoy[3], S. Eidelman[1,32], D. Epifanov[1,32], N. Gabyshev[1,32], A. Garmash[1,32], H. Ha[17], Y. Horii[42], Y. Hoshi[41], W.-S. Hou[27], H. J. Hyun[18], T. Iijima[23], K. Inami[23], A. Ishikawa[35], R. Itoh[9], M. Iwasaki[43], N. J. Joshi[40], D. H. Kah[18], N. Katayama[9], H. Kawai[2], T. Kawasaki[30], H. O. Kim[18], J. H. Kim[38], Y. I. Kim[18], Y. J. Kim[5], B. R. Ko[17], P. Križan[20,15], P. Krokovny[9], R. Kumar[34], A. Kuzmin[1,32], Y.-J. Kwon[47], S.-H. Kyeong[47], M. J. Lee[37], S.-H. Lee[17], T. Lesiak[28,4], A. Limosani[22], C. Liu[36], D. Liventsev[14], R. Louvot[19], A. Matyja[28], S. McOnie[39], H. Miyata[30], R. Mizuk[14], T. Mori[23], Y. Nagasaka[10], S. Nishida[9], O. Nitoh[45], T. Ohshima[23], S. Okuno[16], H. Ozaki[9], P. Pakhlov[14], G. Pakhlova[14], C. W. Park[38], H. K. Park[18], R. Pestotnik[15], L. E. Piilonen[46], A. Poluektov[1,32], Y. Sakai[9], O. Schneider[19], C. Schwanda[13], K. Senyo[23], M. E. Sevior[22], V. Shebalin[1,32], C. P. Shen[8], J.-G. Shiu[27], B. Shwartz[1,32], A. Sokolov[12], S. Stanič[31], M. Starič[15], J. Stypula[28], T. Sumiyoshi[44], G. N. Taylor[22], Y. Teramoto[33], K. Trabelsi[9], S. Uehara[9], Y. Unno[7], S. Uno[9], Y. Usov[1,32], G. Varner[8], K. E. Varvell[39], K. Vervink[19], A. Vinokurova[1,32], C. H. Wang[26], P. Wang[11], Y. Watanabe[16], R. Wedd[22], E. Won[17], B. D. Yabsley[39], H. Yamamoto[42], Y. Yamashita[29], V. Zhilich[1,32], V. Zhulanov[1,32], T. Zivko[15], A. Zupanc[15], O. Zyukova[1,32]

[1]*Budker Institute of Nuclear Physics, Novosibirsk, Russian Federation*
[2]*Chiba University, Chiba, Japan*
[3]*University of Cincinnati, Cincinnati, OH, USA*
[4]*T. Kościuszko Cracow University of Technology, Krakow, Poland*
[5]*The Graduate University for Advanced Studies, Hayama, Japan*
[6]*Gyeongsang National University, Chinju, South Korea*
[7]*Hanyang University, Seoul, South Korea*
[8]*University of Hawaii, Honolulu, HI, USA*
[9]*High Energy Accelerator Research Organization (KEK), Tsukuba, Japan*
[10]*Hiroshima Institute of Technology, Hiroshima, Japan*
[11]*Institute of High Energy Physics, Chinese Academy of Sciences, Beijing, PR China*
[12]*Institute for High Energy Physics, Protvino, Russian Federation*
[13]*Institute of High Energy Physics, Vienna, Austria*
[14]*Institute for Theoretical and Experimental Physics, Moscow, Russian Federation*
[15]*J. Stefan Institute, Ljubljana, Slovenia*
[16]*Kanagawa University, Yokohama, Japan*
[17]*Korea University, Seoul, South Korea*
[18]*Kyungpook National University, Taegu, South Korea*
[19]*École Polytechnique Fédérale de Lausanne, EPFL, Lausanne, Switzerland*
[20]*Faculty of Mathematics and Physics, University of Ljubljana, Ljubljana, Slovenia*
[21]*University of Maribor, Maribor, Slovenia*
[22]*University of Melbourne, Victoria, Australia*
[23]*Nagoya University, Nagoya, Japan*
[24]*Nara Women's University, Nara, Japan*
[25]*National Central University, Chung-li, Taiwan*
[26]*National United University, Miao Li, Taiwan*
[27]*Department of Physics, National Taiwan University, Taipei, Taiwan*
[28]*H. Niewodniczanski Institute of Nuclear Physics, Krakow, Poland*
[29]*Nippon Dental University, Niigata, Japan*
[30]*Niigata University, Niigata, Japan*
[31]*University of Nova Gorica, Nova Gorica, Slovenia*
[32]*Novosibirsk State University, Novosibirsk, Russian Federation*
[33]*Osaka City University, Osaka, Japan*

Preprint submitted to Physics Letters B *November 9, 2009*

[34] *Panjab University, Chandigarh, India*
[35] *Saga University, Saga, Japan*
[36] *University of Science and Technology of China, Hefei, PR China*
[37] *Seoul National University, Seoul, South Korea*
[38] *Sungkyunkwan University, Suwon, South Korea*
[39] *University of Sydney, Sydney, NSW, Australia*
[40] *Tata Institute of Fundamental Research, Mumbai, India*
[41] *Tohoku Gakuin University, Tagajo, Japan*
[42] *Tohoku University, Sendai, Japan*
[43] *Department of Physics, University of Tokyo, Tokyo, Japan*
[44] *Tokyo Metropolitan University, Tokyo, Japan*
[45] *Tokyo University of Agriculture and Technology, Tokyo, Japan*
[46] *IPNAS, Virginia Polytechnic Institute and State University, Blacksburg, VA, USA*
[47] *Yonsei University, Seoul, South Korea*

Abstract

The cross sections for the reactions $e^+e^- \to \phi\eta, \quad \phi\eta', \quad \rho\eta, \quad \rho\eta'$ have been measured using a data sample of 516 fb^{-1} collected with the Belle detector at the KEKB asymmetric-energy e^+e^- collider. The corresponding values of the cross sections are: $1.4 \pm 0.4 \pm 0.1$ fb ($\phi\eta$), $5.3 \pm 1.1 \pm 0.4$ fb ($\phi\eta'$), $3.1 \pm 0.5 \pm 0.1$ fb ($\rho\eta$) and $3.3 \pm 0.6 \pm 0.2$ fb ($\rho\eta'$). The energy dependence of the cross sections is presented using Belle measurements together with those of CLEO and BaBar.

High-statistics data samples accumulated at B-factories allow a study of rare exclusive two-body processes in e^+e^- annihilation. An example of such a highly suppressed process is the reaction $e^+e^- \to VP$, where V and P stand for Vector and Pseudoscalar mesons, respectively. It has been observed [1, 2] that double charm production in $e^+e^- \to J/\psi\eta_c$ has an unexpectedly high cross section. The basic diagram for double charm production is very similar to the one describing $e^+e^- \to \phi\eta(\eta')$ where c quarks are replaced by s quarks. Thus, comparison of the two reactions may contribute to better understanding of the underlying physics. In addition, we investigate the processes $e^+e^- \to \rho\eta(\eta')$, which also belong to the VP class with a different isospin configuration and light quarks only.

Some of the $e^+e^- \to VP$ reactions have previously been measured at different center-of-mass (CM) energies: in the DM1 experiment at $\sqrt{s}$ between 1.4 and 2.18 GeV [3], in the CLEO experiment at $\sqrt{s} = 3.67$ GeV [4] and by the BaBar collaboration at $\sqrt{s}$ between 1 and 3 GeV using initial-state radiation (ISR) [5] and at $\sqrt{s} = 10.58$ GeV [6]. The cross section of the process $e^+e^- \to \rho\eta$ was also measured by the BES collaboration at $\sqrt{s} = 3.65$ GeV [7]. The reaction $e^+e^- \to \phi\eta'$ has not yet been observed, nevertheless the upper limit on its cross section set by CLEO [4] can be useful for discrimination between models that predict different energy dependences.

The QCD-based models predict the energy dependence for the process $e^+e^- \to VP$ to be $1/s^4$ [8, 9] while the cross section for the process $e^+e^- \to \phi\eta$ measured by CLEO and BaBar favors a $1/s^3$ dependence. The form factor for the process $e^+e^- \to VP$ is expected to have a $1/s$ dependence [10]. Recently theoretical calculations of $e^+e^- \to VP$ cross sections have been published, which use the light cone approach [11, 12]. Predictions are given for two values of $\sqrt{s}$: 3.67 and 10.58 GeV. The authors of Ref. [11] claim that their results favor a $1/s^3$ dependence. In Ref. [12] $\sigma \sim 1/s^4$ is expected in the limit $s \to \infty$.

The analysis presented here is based on data taken at the $\Upsilon(4S)$ ($\sqrt{s} = 10.58$ GeV) with the Belle detector at the KEKB asymmetric-energy e^+e^- collider [13]. The total integrated luminosity of the on-resonance sample used in the analysis is 516 fb^{-1}. To check that the processes $e^+e^- \to VP$ are due to a single-photon annihilation and that the hadronic decay of the $\Upsilon(4S)$ does not give a significant contribution, we use a 58 fb^{-1} data sample collected 60 MeV below the resonance peak. All the observed off-resonance signals are consistent with those at the $\Upsilon(4S)$ resonance within statistical errors. We use these data to set upper limits for the branching ratios of $\Upsilon(4S) \to VP$.

A detailed description of the Belle detector is given elsewhere [14]. We mention here only the detector components essential for the present analysis. Charged tracks are reconstructed from hit information in the central drift chamber (CDC) located in a 1.5 T solenoidal magnetic field. Trajectories of charged particles near the collision point are provided by a silicon vertex detector (SVD). Photon detection and energy measurements are performed with a CsI(Tl) electromagnetic calorimeter (ECL). Identification of charged particles is based on the information from the time-of-flight counters (TOF) and silica aerogel Cherenkov counters (ACC). The ACC provides good separation between kaons and pions or muons at momenta above $1.2\,\mathrm{GeV}/c$. The TOF system consists of 128 plastic scintillation counters and is effective in K/π separation for tracks with momenta below $1.2\,\mathrm{GeV}/c$. Low energy kaons are also identified using specific ionization (dE/dx) measurements in the CDC.

In order to identify hadrons, for each of the three hadron types i ($i = \pi,\ K$ and p) a likelihood L_i is formed using information from the ACC, TOF, and dE/dx measurements from the CDC. Kaons are selected with the requirement $L_K/(L_K + L_\pi) > 0.6$, which has an efficiency of 90% and 6% probability to misidentify a pion as a kaon. All charged tracks that are not identified as kaons are considered to be pions.

Signal candidates are selected in two steps. Initially, events with low multiplicity are selected by requiring that the number of charged tracks in an event be two or four with zero net charge and each track have a momentum transverse to the beam axis (p_t) larger than $0.1\,\mathrm{GeV}/c$; and that each track extrapolate to the interaction point (IP) within 1 cm transversely and within 5 cm along the beam direction. To suppress background from Bhabha and $\mu^+\mu^-$ events, the sum of the absolute values of momenta of the first and second highest momentum tracks are required to be less than $9\,\mathrm{GeV}/c$. At least one track with p_t above $0.5\,\mathrm{GeV}/c$ is required. Beam-related background is suppressed by requiring that the position of the reconstructed event vertex be less than 0.5 cm from the IP in the transverse direction and less than 3 cm from the IP along the beam direction.

Photons are defined as ECL clusters with energy deposits above $200\,\mathrm{MeV}$ that are not associated with charged tracks. Neutral pion candidates are formed from pairs of photons with invariant masses in the range 120 to $150\,\mathrm{MeV}/c^2$. The two-photon invariant mass resolution in the mass region of the π^0 is about $6\,\mathrm{MeV}/c^2$. For the $\eta \to \gamma\gamma$ reconstruction we use only photons that do not form a π^0 candidate with any other photon. The invariant mass of $\eta \to \gamma\gamma$ candidates should lie in the range $0.5 - 0.6\,\mathrm{GeV}/c^2$. The two-photon invariant mass resolution in the mass region of the η meson is about $20\,\mathrm{MeV}/c^2$.

After preselection we apply the following requirements to extract the exclusive VP final states:

- The difference between the energy of VP candidates in the CM frame and $\sqrt{s}$ of KEKB should be between -0.3 and $+0.2\,\mathrm{GeV}$;[1]
- The angle between V and P candidates in the CM frame should be larger than 175 degrees.

We consider the following decay modes of vector and pseudoscalar mesons: $\phi(1020) \to K^+K^-$, $\rho \to \pi^+\pi^-$, $\eta \to \gamma\gamma$, $\eta' \to \pi^+\pi^-\gamma$, $\eta' \to \eta\pi^+\pi^-$. After the application of the requirements listed above we observe significant concentrations of events in the scatter plots near the masses of corresponding vector and pseudoscalar mesons. These scatter plots are shown in Figs. 1(a-f).

A two-dimensional unbinned likelihood fit is applied to extract the signal yields for the above reactions. We assume the mass distributions of vector and pseudoscalar particles to be uncorrelated; thus the distributions in the scatter plots of Fig. 1 can be represented as the product of two one-dimensional probability density functions (PDF), one for each dimension.[2] To fit the $\phi(1020) \to K^+K^-$ and $\rho \to \pi^+\pi^-$ invariant mass distributions we use a non-relativistic Breit-Wigner function. The $\eta \to \gamma\gamma$ and $\eta' \to \pi^+\pi^-\gamma$, $\eta\pi^+\pi^-$ invariant mass distributions are fitted with Gaussians. The background for the K^+K^- system is described by the product of the threshold function $(m(K^+K^-) - m_0)^\alpha$ and a first-order polynomial, where α is a free parameter and $m_0 = 2m_{K^+}$. The fit range for $m(K^+K^-)$ extends from m_0 to $1.12\,\mathrm{GeV}/c^2$. The

---

[1] This cut allows for low energy photon radiation up to $0.3\,\mathrm{GeV}$ to be present.

[2] Two-dimentional function thus could be written as: $f(m_1, m_2) = (A\cdot s1 + B\cdot b1)\cdot(C\cdot s2 + D\cdot b2)$, where $s1(m_1)$ and $b1(m_1)$ are one-dimentional signal and background functions for vector particle, $s2(m_2)$ and $b2(m_2)$ – for pseudoscalar particle, A, B, C and D are free fitting parameters.

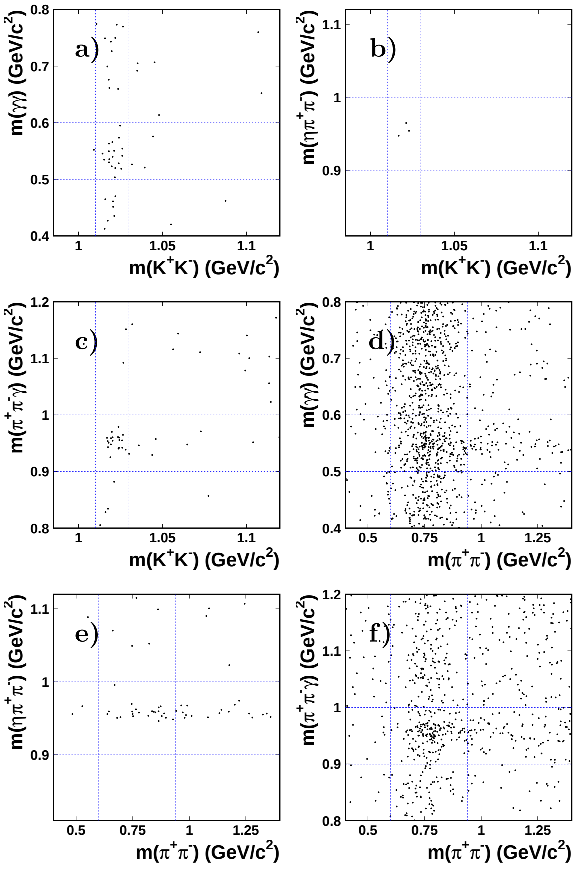

Figure 1: Scatter plots for the processes **a)** $e^+e^- \to \phi\eta \to K^+K^-\gamma\gamma$, **b)** $e^+e^- \to \phi\eta' \to K^+K^-\eta\pi^+\pi^-$, **c)** $e^+e^- \to \phi\eta' \to K^+K^-\pi^+\pi^-\gamma$, **d)** $e^+e^- \to \rho\eta \to \pi^+\pi^-\gamma\gamma$, **e)** $e^+e^- \to \rho\eta' \to \pi^+\pi^-\eta\pi^+\pi^-$, **f)** $e^+e^- \to \rho\eta' \to \pi^+\pi^-\pi^+\pi^-\gamma$. The dotted lines show the mass ranges used for one-dimensional projections.

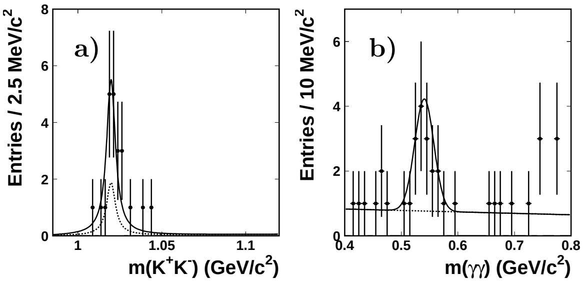

Figure 2: The mass projections for the scatter plot $m(K^+K^-)$ vs. $m(\gamma\gamma)$ onto **a)** K^+K^- and **b)** $\gamma\gamma$ for the reaction $e^+e^- \to \phi\eta \to K^+K^-\gamma\gamma$. The solid curves show the result of the two-dimensional fit, the dotted curves show the background contamination.

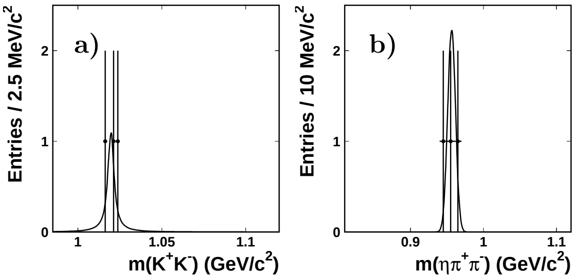

Figure 3: The mass projections for the scatter plot $m(K^+K^-)$ vs. $m(\eta\pi^+\pi^-)$ onto **a)** K^+K^- and **b)** $\eta\pi^+\pi^-$ for the reaction $e^+e^- \to \phi\eta' \to K^+K^-\eta\pi^+\pi^-$. The solid curves show the result of the two-dimensional fit, the dotted curves show the background contamination.

backgrounds for the $\pi^+\pi^-$, $\gamma\gamma$, $\eta\pi^+\pi^-$ and $\pi^+\pi^-\gamma$ systems are parameterized with first-order polynomials. The fit ranges are 0.4–$1.4\,\mathrm{GeV}/c^2$, 0.4–$0.8\,\mathrm{GeV}/c^2$, 0.83–$1.12\,\mathrm{GeV}/c^2$ and 0.8–$1.2\,\mathrm{GeV}/c^2$ for $\pi^+\pi^-$, $\gamma\gamma$, $\eta\pi^+\pi^-$ and $\pi^+\pi^-\gamma$, respectively. The two-dimensional fitting functions for the scatter plots are the sum of products of the corresponding one-dimensional signal and background functions. The mean values (masses) of the signal functions are fixed at PDG values [15] while their widths are fixed to the values obtained from the corresponding inclusive spectra in the data. The significance of the fit is defined as $\sqrt{-2\ln(L_0/L_{\max})}$, where L_0 and $L_{\max}$ are the likelihood values returned by the fit with signal yield fixed to zero and at its best fit value. The signal yields obtained from this fit procedure and the significance of the fits for all processes are presented in Table 1.

The corresponding one-dimensional projections together with the results of a two-dimensional fit for different reactions are shown in Figs. 2(a,b)-7(a,b).

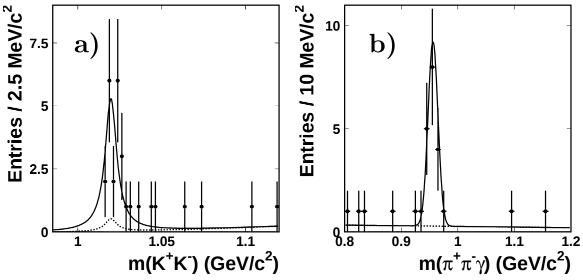

Figure 4: The mass projections for the scatter plot $m(K^+K^-)$ vs. $m(\pi^+\pi^-\gamma)$ onto **a)** K^+K^- and **b)** $\pi^+\pi^-\gamma$ for the reaction $e^+e^- \to \phi\eta' \to K^+K^-\pi^+\pi^-\gamma$. The solid curves show the result of the two-dimensional fit, the dotted curves show the background contamination.

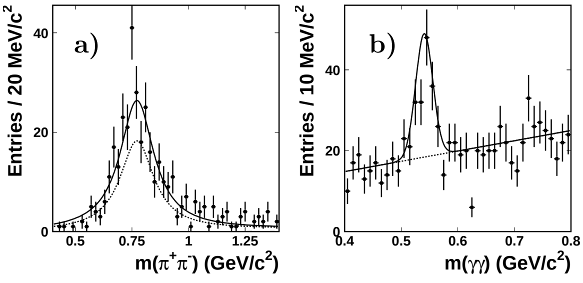

Figure 5: The mass projections for the scatter plot $m(\pi^+\pi^-)$ vs. $m(\gamma\gamma)$ onto **a)** $\pi^+\pi^-$ and **b)** $\gamma\gamma$ for the reaction $e^+e^- \to \rho\eta \to \pi^+\pi^-\gamma\gamma$. The solid curves show the result of the two-dimensional fit, the dotted curves show the background contamination.

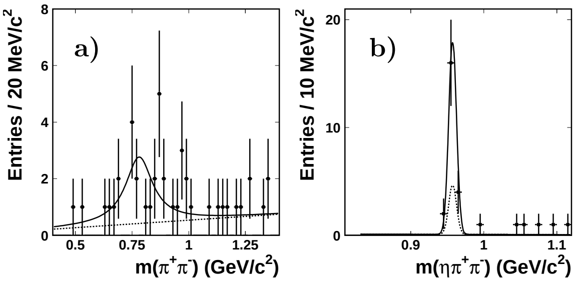

Figure 6: The mass projections for the scatter plot $m(\pi^+\pi^-)$ vs. $m(\eta\pi^+\pi^-)$ onto **a)** $\pi^+\pi^-$ and **b)** $\eta\pi^+\pi^-$ for the reaction $e^+e^- \to \rho\eta' \to \pi^+\pi^-\eta\pi^+\pi^-$. The solid curves show the result of the two-dimensional fit, the dotted curves show the background contamination.

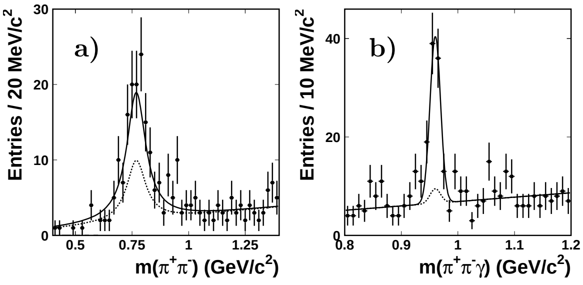

Figure 7: The mass projections for the scatter plot $m(\pi^+\pi^-)$ vs. $m(\pi^+\pi^-\gamma)$ onto **a)** $\pi^+\pi^-$ and **b)** $\pi^+\pi^-\gamma$ for the reaction $e^+e^- \to \rho\eta' \to \pi^+\pi^-\pi^+\pi^-\gamma$. The solid curves show the result of the two-dimensional fit, the dotted curves show the background contamination.

From the fitted signal yields, N, we determine the corresponding cross sections according to the formula:

$$\sigma = \frac{N}{L\, B_V\, B_P\, \varepsilon}, \tag{1}$$

where L is the integrated luminosity (516 fb^{-1}), B_V, B_P are the branching fractions of the corresponding decay channels of the vector and pseudoscalar mesons [15] and ε is the corresponding detection efficiency. The detection efficiencies are determined from Monte Carlo samples where the $e^+e^- \to VP$ reactions are generated without ISR and with an angular dependence corresponding to a $J^P = 1^-$ initial state [16]:

$$\begin{aligned}&\frac{dN}{d\cos\theta^* d\cos\theta_V d\phi_V} \propto \\ &\qquad \sin^2\theta_V(1+\cos^2\theta^* + \cos 2\phi_V \sin^2\theta^*), \end{aligned} \tag{2}$$

with the production angle θ^* defined as the angle between the vector meson direction and incident e^- beam in the CM frame. The vector meson helicity angle θ_V is defined as the polar angle, measured in the vector meson rest frame, of the positive decay product momentum direction with respect to an axis that is aligned with the vector meson momentum direction in the CM frame. The variable ϕ_V is the vector meson's positive decay product azimuthal angle around the direction of the vector meson measured with respect to the plane formed by the vector meson and the incoming electron. The generated events were passed through a full GEANT [17] Belle simulation and reconstruction procedures including the trigger simulation. The trigger efficiencies, estimated with MC samples described above, are about 93% and over

Table 1: Observed number of events, significance (Σ) of the fit, efficiencies and cross sections (σ).

Process	N_{signal}	Σ	ε, **%**	σ, **fb**
$\phi\eta(\gamma\gamma)$	14.6 ± 4.3	8.0	14.1	1.1 ± 0.3
$\phi\eta'(\eta\pi^+\pi^-)$	3.0 ± 1.7	12.0	0.917	2.9 ± 1.6
$\phi\eta'(\pi^+\pi^-\gamma)$	19.6 ± 4.5	30.0	5.36	4.9 ± 1.1
$\phi\eta'$(comb.)				4.3 ± 0.9
$\rho\eta(\gamma\gamma)$	116.3 ± 20.2	9.2	23.2	2.5 ± 0.4
$\rho\eta'(\eta\pi^+\pi^-)$	17.9 ± 4.8	7.9	3.58	2.2 ± 0.6
$\rho\eta'(\pi^+\pi^-\gamma)$	72.1 ± 15.0	7.6	14.3	3.3 ± 0.7
$\rho\eta'$(comb.)				2.7 ± 0.5

Table 2: Total systematic uncertainties for analyzed channels.

Channel	**Error (%)**
$e^+e^- \to \phi\eta \to K^+K^-\gamma\gamma$	5.3
$e^+e^- \to \phi\eta' \to K^+K^-\gamma\gamma\pi^+\pi^-$	7.4
$e^+e^- \to \phi\eta' \to K^+K^-\pi^+\pi^-\gamma$	6.2
$e^+e^- \to \rho\eta \to \pi^+\pi^-\gamma\gamma$	5.0
$e^+e^- \to \rho\eta' \to \pi^+\pi^-\gamma\gamma\pi^+\pi^-$	7.0
$e^+e^- \to \rho\eta' \to \pi^+\pi^-\pi^+\pi^-\gamma$	5.9

97% for two-charged-track and four-charged-track events, respectively.

The cross sections before applying radiative corrections together with the observed numbers of signal events, significances of the fit and efficiencies are presented in Table 1. Efficiencies for the processes $e^+e^- \to \phi\eta'(\eta\pi^+\pi^-)$ and $e^+e^- \to \rho\eta'(\eta\pi^+\pi^-)$ include the branching fraction of $\eta \to \gamma\gamma$ $(39.31 \pm 0.20)\%$ [15].

The systematic uncertainty on the $\eta \to \gamma\gamma$ detection efficiency is dominated by the uncertainty on the MC shower simulation in the ECL and other material. In order to estimate this uncertainty, we compare the ratio of signal yields for the decays $\eta \to \gamma\gamma$ and $\eta \to \pi^0\pi^0\pi^0$ in the data and in Monte Carlo simulation. We observe a difference of about 4%, which is treated as the systematic error in the $\eta \to \gamma\gamma$ detection efficiency. We assume the uncertainty in the single photon detection efficiency to be 2%. The systematic uncertainties due to the experimenta errors in the branching fractions of the analyzed decay channels [15] are 1.3%, 3.4%, 0.5% and 3.2% for the $\phi\eta$, $\phi\eta'$, $\rho\eta$ and $\rho\eta'$, respectively. The systematic uncertainty in the tracking efficiency is estimated from $D^{*+} \to D^0\pi^+ \to K^-\pi^+\pi^+$ decays to be 1% per track. The systematic uncertainty from the two-dimensional fit is estimated from variations in the number of events with mass values and widths floating and fixed. It is estimated to be 1.5%. The uncertainty in the luminosity measurement is determined by the accuracy of the Bhabha generator, which is 1.4%. The systematic uncertainty due to trigger efficiency is obtained from comparison of the rate of the $e^+e^- \to \phi\gamma$ events with the one expected from MC simulation. It is taken to be 1%. The uncertainty due to limited Monte Carlo statistics is at most 2% for the process $e^+e^- \to \phi\eta' \to K^+K^-\gamma\gamma\pi^+\pi^-$. The uncertainty on the charged kaon identification is estimated by comparing efficiencies of kaon identification in decays $D^{*+} \to D^0\pi^+ \to K^-\pi^+\pi^+$ for the data and Monte Carlo events. For the uncertainty of a charged kaon identification we take the relative difference in these efficiencies, which is 0.5% per kaon. The systematic uncertainties for all analyzed channels are given in Table 2.

To check whether the observed signals are due to $\Upsilon(4S)$ decays, we scale the off-resonance signals to the on-resonance luminosity, and subtract them from the on-resonance signals. The observed numbers of events in the off-resonance data are 1 ± 1, 1 ± 1, 2 ± 1.4, 15.2 ± 4.7, 1 ± 1, 7 ± 3.6 for the processes $\phi\eta(\gamma\gamma)$, $\phi\eta'(\eta\pi^+\pi^-)$, $\phi\eta'(\pi^+\pi^-\gamma)$, $\rho\eta(\gamma\gamma)$, $\rho\eta'(\eta\pi^+\pi^-)$ and $\rho\eta'(\pi^+\pi^-\gamma)$, respectively. The resulting branching fractions for $\Upsilon(4S) \to VP$ are $(0.4 \pm 0.8) \times 10^{-6}$, $(-0.6 \pm 2.8) \times 10^{-6}$, $(-0.5 \pm 1.0) \times 10^{-6}$, $(0.8 \pm 0.9) \times 10^{-6}$ for the $\phi\eta$, $\phi\eta'$, $\rho\eta$, $\rho\eta'$ channels, respectively, which are consistent with zero. These results can be expressed as the 90% confidence level upper limits [18], which are equal to 1.8×10^{-6}, 4.3×10^{-6}, 1.3×10^{-6}, 2.5×10^{-6} for the $\phi\eta$, $\phi\eta'$, $\rho\eta$, $\rho\eta'$ channels, respectively. The systematic uncertainties are also taken into account for upper limit calculations

In the light cone approach the authors of Refs. [11, 12] gave predictions for the cross sections of the reactions analyzed by Belle at $\sqrt{s} = 10.58\,\text{GeV}$. In Table 3 we present the Belle cross sections radiatively corrected according to Ref. [19] together with theory predictions [11, 12]. The radiatively corrected cross section can be written as

$$\sigma_0 = \frac{\sigma}{1+\delta}, \tag{3}$$

where σ is taken from equation (1). The value of

$1+\delta$ corresponding to the energy cut of 0.3 GeV is equal to 0.809 [19]. The BaBar measurement of the reaction $e^+e^- \to \phi\eta$ [6] is also presented in the table. The corresponding value of $1+\delta$ for the BaBar energy cut of 0.23 GeV is 0.768. BaBar reports that the cross section of the reaction $e^+e^- \to \phi\eta$ is $2.9 \pm 0.5 \pm 0.1$ fb [6]. The Belle cross section is smaller than the BaBar result by about 2.3σ.

From Table 3 we see that in comparison to theory [11, 12] the Belle experimental cross section for $e^+e^- \to \phi\eta$ is significantly lower, $e^+e^- \to \rho\eta'$ is about 1.8σ higher, while $e^+e^- \to \phi\eta'$ and $e^+e^- \to \rho\eta$ agree within errors with theory. There is also a discrepancy between the data and light cone expectation in the ratio of the cross section of η meson production together with vector mesons to that of η' production. As can be seen from Table 3, the light cone approach [11] predicts $\frac{\sigma(e^+e^-\to\rho\eta)}{\sigma(e^+e^-\to\rho\eta')} > 1$ while this trend is not observed in data.

The energy dependence of the cross sections may have important theoretical implications. In Figs. 8(a-d) we show the Belle data radiatively corrected according to Ref. [19] together with CLEO and BaBar ISR results. The BaBar data were averaged for $\sqrt{s}$ values from 2.5 to 3 GeV. We also show $1/s^3$ and $1/s^4$ dependences, which pass through the CLEO points. In Fig. 8(b) the arrow shows the CLEO upper limit and the curves pass through the Belle measurement. From Fig. 8 we cannot draw any definite conclusion about the energy dependence of the $e^+e^- \to VP$ reactions.

To summarize, we have measured cross sections of the exclusive processes $e^+e^- \to \phi\eta$, $e^+e^- \to \phi\eta'$, $e^+e^- \to \rho\eta$, $e^+e^- \to \rho\eta'$ where the final state includes soft photons with energies below 0.3 GeV using a 516 fb^{-1} data sample recorded near $\sqrt{s} = 10.58$ GeV. The corresponding values of the cross sections in femtobarns are: $1.4 \pm 0.4 \pm 0.1$, $5.3 \pm 1.1 \pm 0.4$, $3.1 \pm 0.5 \pm 0.1$ and $3.3 \pm 0.6 \pm 0.2$. The results are compared with theoretical predictions from the light cone approach [11, 12]. Analysis of the energy dependence of the cross sections using our results together with those of CLEO at $\sqrt{s} = 3.67$ GeV [4] and BaBar 2.5 GeV for $\phi\eta$ and 2.75 GeV for $\rho\eta$, $\rho\eta'$ [5] shows that there is no universal energy dependence for these processes. The ratios of cross sections of η meson production together with vector mesons to the corresponding cross sections for η' meson production are different from the light cone expectation [11, 12]. The 90% confidence level upper limits on the branching fractions of the $\Upsilon(4S) \to VP$ are 1.8×10^{-6}, 4.3×10^{-6}, 1.3×10^{-6}, 2.5×10^{-6} for the $\phi\eta$, $\phi\eta'$, $\rho\eta$, $\rho\eta'$ channels, respectively.

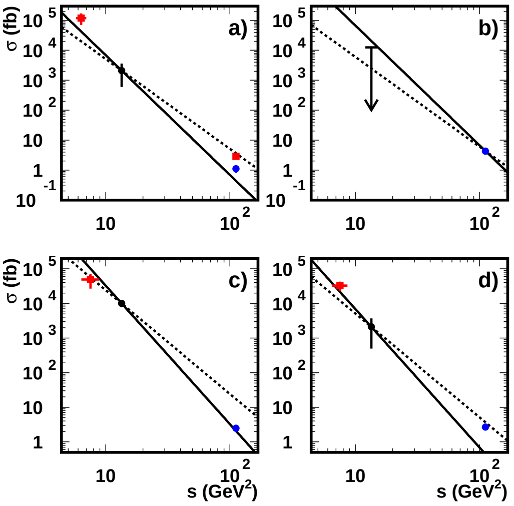

Figure 8: The measured cross sections at $\sqrt{s} \approx 2.5$, 2.75 GeV by BaBar, $\sqrt{s} = 3.67$ GeV by CLEO and at $\sqrt{s} = 10.58$ GeV by BaBar and Belle for the various processes. BaBar measurements are represented by squares. **a)** $e^+e^- \to \phi\eta$, **b)** $e^+e^- \to \phi\eta'$; **c)** $e^+e^- \to \rho\eta$; **d)** $e^+e^- \to \rho\eta'$. In the plot b) the CLEO upper limit is shown by the arrow. The solid lines correspond to a $1/s^4$ dependence and the dashed ones represent $1/s^3$.

We thank the KEKB group for the excellent operation of the accelerator, the KEK cryogenics group for the efficient operation of the solenoid, and the KEK computer group and the National Institute of Informatics for valuable computing and SINET3 network support. We acknowledge support from the Ministry of Education, Culture, Sports, Science, and Technology (MEXT) of Japan, the Japan Society for the Promotion of Science (JSPS), and the Tau-Lepton Physics Research Center of Nagoya University; the Australian Research Council and the Australian Department of Industry, Innovation, Science and Research; the National Natural Science Foundation of China under contract No. 10575109, 10775142, 10875115 and 10825524; the Department of Science and Technology of India; the BK21 program of the Ministry of Education of Korea, the CHEP src program and Basic Research program (grant No. R01-2008-000-10477-0) of the Korea Science and Engineering Foundation; the Polish Ministry of Science and Higher Education; the Ministry of Education and Science of the Russian Federa-

Table 3: The values of cross sections of reactions $e^+e^- \to VP$, radiatively corrected according to Ref. [19], measured by Belle and predicted by theory [11, 12] and the BaBar measurement.

Channel	σ_0 **Belle (fb)**	σ **[11] (fb)**	σ **[12] (fb)**	σ_0 **BaBar (fb)**
$e^+e^- \to \phi\eta$	$1.4 \pm 0.4 \pm 0.1$	$3.3 - 4.3$	$2.4 - 3.4$	$2.9 \pm 0.5 \pm 0.1$
$e^+e^- \to \phi\eta'$	$5.3 \pm 1.1 \pm 0.4$	$4.4 - 5.8$	$3.5 - 5.0$	–
$e^+e^- \to \rho\eta$	$3.1 \pm 0.5 \pm 0.1$	$2.4 - 3.1$	$2.4 - 3.5$	–
$e^+e^- \to \rho\eta'$	$3.3 \pm 0.6 \pm 0.2$	$1.5 - 2.1$	$1.6 - 2.3$	–

tion and the Russian Federal Agency for Atomic Energy; the Slovenian Research Agency; the Swiss National Science Foundation; the National Science Council and the Ministry of Education of Taiwan; and the U.S. Department of Energy. This work is supported by a Grant-in-Aid from MEXT for Science Research in a Priority Area ("New Development of Flavor Physics"), and from JSPS for Creative Scientific Research ("Evolution of Tau-lepton Physics").

References

- [1] K.Abe *et al.* (Belle Collaboration), Phys. Rev. Lett. **89**, 142001 (2002); Phys. Rev. D **70**, 071102 (2004).
- [2] B. Aubert *et al.* (BaBar Collaboration), Phys. Rev. D **72**, 031101 (2005).
- [3] B. Delcourt *et al.* (DM1 Collaboration), Phys. Lett. B **113**, 93 (1982); Erratim-ibid. B **115**, 503 (1982).
- [4] G.S. Adams *et al.* (CLEO Collaboration), Phys. Rev. D **73**, 012002 (2006).
- [5] B. Aubert *et al.* (BaBar Collaboration), Phys. Rev. D **76**, 092005 (2007).
- [6] B. Aubert *et al.* (BaBar Collaboration), Phys. Rev. D **74**, 111103(R) (2006).
- [7] M. Ablikim *et al.* (BES Collaboration), Phys. Rev. D **70**, 112007 (2004).
- [8] G.P. Lepage and S.J. Brodsky, Phys. ReV. D **22**, 2157 (1980); S.J. Brodsky and G.P. Lepage, Phys. Rev. D **24**, 2848 (1981).
- [9] V. Chernyak, hep-ph/9906387; V.L. Chernyak and A.R. Zhitnitsky, Phys. Rep. **112**, 173 (1984).
- [10] J.M. Gérard and G. López Castro, Phys. Lett. B **425**, 365 (1998).
- [11] Cai-Dian Lü, Wei Wang and Yu-Ming Wang, Phys. Rev. D **75**, 094020 (2007).
- [12] V.V. Braguta, A.K. Likhoded, A.V. Luchinsky, Phys. Rev. D **78**, 074032 (2008).
- [13] S. Kurokawa and E. Kikutani, Nucl. Instrum. Methods Phys. Res. Sect. A **499**, 1 (2003), and other papers included in this Volume.
- [14] A. Abashian *et al.*. (Belle Collaboration), Nucl. Instrum. Methods Phys. Res. Sect. A **479**, 117 (2002).
- [15] C. Amsler *et al.* (Particle Data Group), Phys. Lett. B **667**, 1 (2008).
- [16] M. Jacob and G.C. Wick, Ann. Phys. **7**, 404 (1959); S.U. Chung, Phys. Rev. D **57**, 431 (1998).
- [17] R. Brun, R. Hagelberg, M. Hansroul, and J.C. Lassalle, "GEANT: Simulation program for Particle Physics Experiments. User Guide and Reference Manual", CERN-DD-78-2-REV 1 (1978).
- [18] G.J. Feldman and R.D. Cousins, Phys. Rev. D **57**, 3873 (1998).
- [19] M. Benayoun, S.I. Eidelman, V.N. Ivanchenko, and Z.K. Silagadze, Mod. Phys. Lett. A **14**, 2605 (1999).